MITSUBISHI ELECTRIC RESEARCH LABORATORIES
https://www.merl.com

quEEGNet: Quantum AI for Biosignal Processing

Koike-Akino, Toshiaki; Wang, Ye

TR2022-121 October 04, 2022

Abstract

In this paper, we introduce an emerging quantum machine learning (QML) framework to assist classical deep learning methods for biosignal processing applications. Specif- ically, we propose a hybrid quantum-classical neural network model that integrates a variational quantum circuit (VQC) into a deep neural network (DNN) for electroencephalogram (EEG), electromyogram (EMG), and electrocorticogram (ECoG) analysis. We demonstrate that the proposed quantum neural network (QNN) achieves state-of-the-art performance while the number of trainable parameters is kept small for VQC.

IEEE Conference on Biomedical and Health Informatics (BHI) 2022

Mitsubishi Electric Research Laboratories, Inc.
201 Broadway, Cambridge, Massachusetts 02139

quEEGNet: Quantum AI for Biosignal Processing

Toshiaki Koike-Akino, Ye Wang
Mitsubishi Electric Research Laboratories (MERL)
201 Broadway, Cambridge, MA 02139, USA
{koike, yewang}@merl.com

***Abstract*—In this paper, we introduce an emerging quantum machine learning (QML) framework to assist classical deep learning methods for biosignal processing applications. Specifically, we propose a hybrid quantum-classical neural network model that integrates a variational quantum circuit (VQC) into a deep neural network (DNN) for electroencephalogram (EEG), electromyogram (EMG), and electrocorticogram (ECoG) analysis. We demonstrate that the proposed quantum neural network (QNN) achieves state-of-the-art performance while the number of trainable parameters is kept small for VQC.**

***Index Terms*—Quantum computing, deep neural network (DNN), quantum machine learning (QML), electroencephalogram (EEG), electromyogram (EMG), biosignal processing**

I. Introduction

The great advancement of artificial intelligence (AI) techniques based on deep neural networks (DNN) has enabled practical development of human-machine interfaces (HMI) including brain-computer interfaces (BCI) through the analysis of the user's physiological data [1], such as electroencephalogram (EEG) [2] and electromyogram (EMG) [3]. However, such biosignals are highly prone to variation depending on the biological states of each subject [4]. Hence, frequent calibration is often required in typical HMI systems. Toward resolving this issue, subject-invariant methods [5]–[11], employing domain generalization and transfer learning, have been proposed to reduce user calibration for HMI systems.

In this paper, we introduce an emerging framework "quantum machine learning (QML)" [12]–[31] into biosignal processing applications for the first time in the literature, envisioning future era of *quantum supremacy* [32], [33]. Quantum computers have the potential to realize computationally efficient signal processing compared to traditional digital computers by exploiting quantum mechanisms, e.g., superposition and entanglement, in terms of not only execution time but also energy consumption. In the past few years, several vendors have successfully manufactured commercial quantum processing units (QPUs). For instance, IBM released 127-qubit QPUs in 2021, and plans to produce 1121-qubit QPUs by 2023. It is thus no longer far future when QML will be widely used for real applications. Recently, hybrid quantum-classical algorithms based on the *variational* principle [34]–[37] were proposed to deal with quantum noise.

The main contributions of this paper are summarized below:

- We introduce the emerging QML framework for biosignal processing;
- We propose a hybrid quantum-classic DNN model called *quEEGNet*;
- We demonstrate the proof-of-concept study on QML for various physiological datasets.

To the best of our knowledge, this is the very first research on QML applied to HMI and BCI fields. Although there exist a few literature [38], [39] discussing the potential use of quantum computing for BCI, no practical demonstration on QML-assisted HMI systems is found to date. Note that our QNN is different from a recurrent QNN (RQNN) employing quantum stochastic filtering based on the Schrödinger equation [40]–[43], which is motivated by quantum physics but does not need real QPUs. In addition, our work is tangential to quantum sensing technologies such as superconducting quantum interference devices (SQUID) [44].

II. Quantum Artificial Intelligence (QAI) for HMI

A. Quantum Bit (Qubit)

In quantum systems, a *qubit* is expressed as the following state superposing bases of $|0\rangle$ and $|1\rangle$: $|\phi\rangle = \alpha_0|0\rangle + \alpha_1|1\rangle$, where α_1 and α_2 are complex numbers subject to $|\alpha_0|^2 + |\alpha_1|^2 = 1$. When qubits are measured, the classical bit 0 or 1 is observed with a probability of $|\alpha_0|^2$ or $|\alpha_1|^2$, respectively. The above *ket-notation* corresponds to column-vector operations of the two basis states $|0\rangle = [1, 0]^{\mathrm{T}}$ and $|1\rangle = [0, 1]^{\mathrm{T}}$, whereas the *bra-notation* is used for row-vector operations corresponds to its Hermitian transpose; i.e., $\langle\phi| = |\phi\rangle^{\dagger} = [\alpha_0^*, \alpha_1^*]$. Here, $[\cdot]^{\dagger}$, $[\cdot]^*$ and $[\cdot]^{\mathrm{T}}$ denote Hermitian transpose, complex conjugate and transpose, respectively. Note that a multi-qubit state is represented by sum of Kronecker products of basis vectors such as $|000\rangle = |0\rangle^{\otimes 3}$.

B. Quantum Gates

The basic operations on a qubit is defined as a unitary matrix, which is called *gate*. Some of the most common gates are associated with Pauli matrices: $\mathbf{I} = \left[\begin{smallmatrix} 1 & 0 \\ 0 & 1 \end{smallmatrix}\right]$, $\mathbf{X} = \left[\begin{smallmatrix} 0 & 1 \\ 1 & 0 \end{smallmatrix}\right]$, $\mathbf{Y} = \left[\begin{smallmatrix} 0 & -\jmath \\ \jmath & 0 \end{smallmatrix}\right]$, and $\mathbf{Z} = \left[\begin{smallmatrix} 1 & 0 \\ 0 & -1 \end{smallmatrix}\right]$, where $\jmath$ is the imaginary unit satisfying $\jmath^2 = -1$. The X gate is bit-flip (i.e., NOT operation), Z gate is phase-flip, and Y gate flips both bit and phase. The Hadamard (H) gate is used to generate a superposition state $|+\rangle = \frac{1}{\sqrt{2}}|0\rangle + \frac{1}{\sqrt{2}}|1\rangle$: $\mathbf{H} = \frac{1}{\sqrt{2}}\left[\begin{smallmatrix} 1 & 1 \\ 1 & -1 \end{smallmatrix}\right]$. A controlled-NOT (CNOT or CX) gate is a multi-qubit gate that flips the target qubit if and only if the control qubit is $|1\rangle$.

C. Quantum Machine Learning (QML)

A number of modern DNN methods have been already migrated into the quantum domain, e.g., convolutional layers [12], autoencoders [13], graph neural networks [17], and

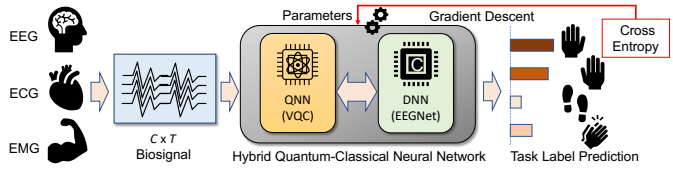

Fig. 1. Hybrid quantum-classical neural networks for biosignal processing.

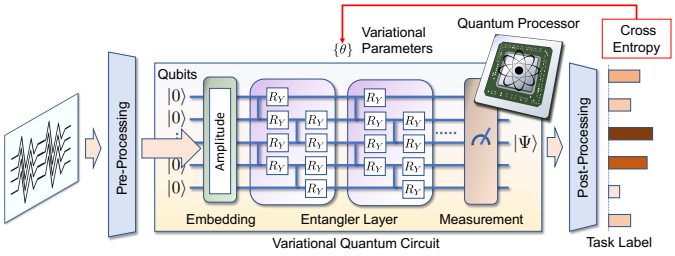

Fig. 2. Variational QNN for HMI systems.

generative adversarial networks [15], [16]. Interestingly, the number of QML articles has been exponentially increasing at the same rate of DNN articles, doubling every year, but just 6 years behind [28]. It suggests that QML will be potentially used in numerous communities in a couple of years. In fact, real QPUs are readily accessible through a cloud quantum server such as IBM QX and Amazon braket.

In analogy with DNN, it was proved that QNN holds the universal approximation property [45]. Accordingly, increasing the number of qubits and quantum layers may enjoy state-of-the-art DNN performance. In addition, quantum circuits are analytically differentiable [46], enabling stochastic gradient optimization of QNN. Nevertheless, QNN often suffers from a vanishing gradient issue called the barren plateau [47]. To mitigate the issue, a simplified 2-design (S2D) ansatz [19] was proposed to realize shallow entanglers for arbitrary unitary approximation. It is highly expected that quantum computers would offer breakthroughs in a wide range of fields.

D. Quantum Neural Network (QNN) for HMI

Fig. 1 shows an HMI system employing quantum-classical neural network model for biosignal processing. The system feeds biological waveform arrays to predict a task label through a neural network, which integrates a QNN model with a classical DNN model such as EEGNet [2]. The variational parameters for QNN and other trainable parameters for DNN are jointly optimized by stochastic gradient methods to minimize a loss function in an iterative manner.

Fig. 2 depicts an exemplar QNN model based on VQC employing the S2D ansatz [19], which consists of Pauli-Y rotations and staggered controlled-Z entanglers, to evolve the quantum states. This ansatz is a simplified variant of a 2-design whose statistical properties are identical to ensemble random unitaries with respect to the Haar measure up to the first 2 moments. For an n-qubit variational quantum circuit, there are $2(n-1)L$ variational parameters $\{\theta\}$ over an L-layer S2D ansatz.

To feed multi-dimensional data, an input layer based on batch normalization is used to initialize the quantum state through the use of an amplitude embedding, which enables encoding up to $2^n - 1$ values for n-qubit QPUs. The multi-label task prediction is provided by quantum measurements in the Hamiltonian observable of Pauli-Z operations, followed by a post-processing layer to align the dimension. The variational parameters as well as input/output layers are optimized by a gradient method to minimize the softmax cross entropy loss. While QNN is not necessarily better than DNN in prediction accuracy, it can be computationally efficient by manipulating exponentially many quantum states in parallel with a small number of quantum gates.

We integrate the QNN with EEGNet, where the QNN performs as feature extraction and EEGNet works as the post-processing layers. Note that various other different combinations are possible, e.g., two individual VQC layers for temporal and spatial convolutions; VQC in recurrent networks. We refer to all such hybrid QNN+DNN concepts (not specific architectures) suited for biological analysis as a *quantum EEGNet (quEEGNet)* by convention.

TABLE I
PARAMETERS OF PUBLIC DATASET UNDER INVESTIGATION

Dataset	Modality	Dimension	Subjects	Classes	Samples
Stress [48]	Temp. etc.	7×1	20	4	24,000
RSVP [49]	EEG	16×128	10	4	41,400
MI [50]	EEG	64×480	106	4	9,540
ErrP [51]	EEG	56×250	27	2	9,180
Faces Basic [52]	ECoG	31×400	14	2	4,100
Faces Noisy [53]	ECoG	39×400	7	2	2,100
ASL [54]	EMG	16×50	5	33	9,900

III. EXPERIMENTAL EVALUATION

A. Datasets

We use publicly available physiological datasets, summarized in Table I. These cover a wide variety of data size, dimensionality, and subject scale as well as sensor modalities, including EEG, EMG, and electrocorticography (ECoG).

1) Stress: A physiological dataset for neurological stress level [48].[1] It consists of multi-modal biosignals for 4 discrete stress states (physical/cognitive/emotional stresses and relaxation) from 20 healthy subjects. The data collection consisted of 7 dimensions of multi-model sensing, i.e., electrodermal activity, temperature, three-dimensional acceleration, heart rate, and arterial oxygen level. A task of 5 minutes long ($T = 300$ time samples with 1 Hz down-sampling) was executed for a total of 4 trials per state.

2) RSVP: An EEG-based typing interface using a rapid serial visual presentation (RSVP) paradigm [49].[2] 10 healthy subjects participated in the experiments at three sessions performed on different days. The dataset consists of 16-channel EEG data for $T = 128$ samples, which were collected by a

[1]Stress dataset: https://physionet.org/content/noneeg/1.0.0/
[2]RSVP dataset: http://hdl.handle.net/2047/D20294523

g.USBamp amplifier with active electrodes during keyboard operations, for 4 labels of emotion elicitation, resting-state, or motor imagery/execution task.

3) MI: The PhysioNet EEG motor imagery (MI) dataset [50].[3] Excluding irregular timestamps, the dataset consists of 106 subjects' EEG data. The subjects were instructed to perform cue-based motor execution/imagery tasks while 64 channels were recorded at a sampling rate of 160 Hz. We use the EEG data for three seconds of post-cue interval data ($T = 480$ time samples). The subject performed 4-class tasks: right hand motor imagery; left hand motor imagery; both hands motor imagery; or both feet motor imagery.

4) ErrP: An error-related potential (ErrP) EEG dataset [51].[4] The dataset consists of EEG data recorded from 16 healthy subjects in an offline P300 spelling task, where visual feedback of the inferred letter is provided at the end of each trial for 1.3 seconds to monitor evoked brain responses for erroneous decisions made by the system. EEG data were recorded from 56 channels for epoched 1.25 seconds at a sampling rate of 200 Hz ($T = 250$). Across 5 recording sessions, each subject performed a total of 340 trials.

5) Faces Basic: An implanted ECoG array dataset for visual stimulus experiments [52], [53].[5] ECoG arrays were implanted on the subtemporal cortical surface of 14 epilepsy patients. 2 classes of grayscale images, either faces or houses, were displayed rapidly in random sequence for 400 ms. The ECoG potentials were measured with respect to a scalp reference and ground, at a sampling rate of 1000 Hz. Subjects performed a basic face-vs-house discrimination task. We use the first 31 channels to analyze for $T = 400$.

6) Faces Noisy: The implanted ECoG arrays dataset for visual stimulus experiments [52], [55]. The experiment is similar to Faces Basic dataset, while pictures of faces and houses are randomly scrambled. There are 7 subjects with 39 channels. Refer ethics statement to reuse the dataset.

7) ASL: An EMG dataset for finger gesture identification for American Sign Language (ASL) [54].[6] 5 healthy, right-handed, subjects participated in experiments with surface EMG (Delsys Trigno) recorded at 2 kHz from 16 lower-arm muscles. Subjects shaped their right hand into an ASL posture presented on a video screen (33 postures, 3 trials per posture). Dynamic letters 'J' and 'Z' were omitted, along with the number '0', which is confusing with the letter 'O'. The participants were given 2 seconds to form the posture and 6 seconds to maintain. The signal is decimated to be $T = 50$.

B. Model Implementation

We use PennyLane and PyTorch libraries to train quEEGNet. The trainable parameters are optimized by the adaptive momentum (Adam) with a learning rate of 0.1 for 50 epochs with a batch size of 128.

[3]MI dataset: https://physionet.org/physiobank/database/eegmmidb/

[4]ErrP dataset: https://www.kaggle.com/c/inria-bci-challenge/

[5]Faces dataset: https://exhibits.stanford.edu/data/catalog/zk881ps0522

[6]ASL Dataset: http://hdl.handle.net/2047/D20294523

TABLE II
PERFORMANCE RESULTS IN TEST ACCURACY (%)

Dataset	EEGNet	quEEGNet
Stress	85.87	87.23
RSVP	93.73	95.12
MI	59.61	60.22
ErrP	74.36	75.92
Faces Basic	63.30	64.92
Faces Noisy	75.94	78.01
ASL	23.64	25.16

C. Performance Results

Table II shows the performance comparison between EEGNet and quEEGNet. It was verified that the hybrid quantum-classical model outperforms classical neural networks for all of the physiological datasets. Since we have not explored different variants of quantum ansatz yet, it is expected that the performance can be further improved via AutoQML [30].

IV. CONCLUSIONS

We proposed an emerging QML framework for HMI/BCI systems, considering the recent rapid advancement of quantum technology. Our hybrid quantum-classical neural network was demonstrated to achieve the state-of-the-art performance for various physiological datasets. As the application of QML to HMI/BCI fields is still at a proof-of-concept phase, there remain many open problems to explore for future work.

REFERENCES

[1] O. Faust, Y. Hagiwara, T. J. Hong, O. S. Lih, and U. R. Acharya, "Deep learning for healthcare applications based on physiological signals: A review," *Computer methods and programs in biomedicine*, vol. 161, pp. 1–13, 2018.

[2] V. J. Lawhern, A. J. Solon, N. R. Waytowich, S. M. Gordon, C. P. Hung, and B. J. Lance, "EEGNet: a compact convolutional neural network for EEG-based brain–computer interfaces," *Journal of neural engineering*, vol. 15, no. 5, p. 056013, 2018.

[3] M. Atzori, M. Cognolato, and H. Müller, "Deep learning with convolutional neural networks applied to electromyography data: A resource for the classification of movements for prosthetic hands," *Frontiers in neurorobotics*, vol. 10, p. 9, 2016.

[4] C. Vidaurre and B. Blankertz, "Towards a cure for BCI illiteracy," *Brain topography*, vol. 23, no. 2, pp. 194–198, 2010.

[5] D. Wu, Y. Xu, and B.-L. Lu, "Transfer learning for EEG-based brain–computer interfaces: A review of progress made since 2016," *IEEE Transactions on Cognitive and Developmental Systems*, vol. 14, no. 1, pp. 4–19, 2020.

[6] A. Demir, T. Koike-Akino, Y. Wang, and D. Erdogmus, "AutoBayes: Automated Bayesian graph exploration for nuisance-robust inference," *IEEE Access*, vol. 9, pp. 39 955–39 972, 2021.

[7] O. Özdenizci, Y. Wang, T. Koike-Akino, and D. Erdoğmuş, "Adversarial deep learning in EEG biometrics," *IEEE signal processing letters*, vol. 26, no. 5, pp. 710–714, 2019.

[8] ——, "Transfer learning in brain-computer interfaces with adversarial variational autoencoders," in *2019 9th International IEEE/EMBS Conference on Neural Engineering (NER)*. IEEE, 2019, pp. 207–210.

[9] M. Han, O. Özdenizci, Y. Wang, T. Koike-Akino, and D. Erdoğmuş, "Disentangled adversarial autoencoder for subject-invariant physiological feature extraction," *IEEE signal processing letters*, vol. 27, pp. 1565–1569, 2020.

[10] M. Han, O. Özdenizci, T. Koike-Akino, Y. Wang, and D. Erdoğmuş, "Universal physiological representation learning with soft-disentangled rateless autoencoders," *IEEE Journal of Biomedical and Health Informatics*, vol. 25, no. 8, pp. 2928–2937, 2021.

[11] N. Smedemark-Margulies, Y. Wang, T. Koike-Akino, and D. Erdogmus, "AutoTransfer: Subject transfer learning with censored representations on biosignals data," *arXiv preprint arXiv:2112.09796*, 2021.

[12] M. Henderson, S. Shakya, S. Pradhan, and T. Cook, "Quanvolutional neural networks: powering image recognition with quantum circuits," *Quantum Machine Intelligence*, vol. 2, no. 1, pp. 1–9, 2020.

[13] J. Romero, J. P. Olson, and A. Aspuru-Guzik, "Quantum autoencoders for efficient compression of quantum data," *Quantum Science and Technology*, vol. 2, no. 4, p. 045001, 2017.

[14] P. Rebentrost, M. Mohseni, and S. Lloyd, "Quantum support vector machine for big data classification," *Physical review letters*, vol. 113, no. 13, p. 130503, 2014.

[15] S. Lloyd and C. Weedbrook, "Quantum generative adversarial learning," *Physical review letters*, vol. 121, no. 4, p. 040502, 2018.

[16] P.-L. Dallaire-Demers and N. Killoran, "Quantum generative adversarial networks," *Physical Review A*, vol. 98, no. 1, p. 012324, 2018.

[17] G. Verdon, T. McCourt, E. Luzhnica, V. Singh, S. Leichenauer, and J. Hidary, "Quantum graph neural networks," *arXiv preprint arXiv:1909.12264*, 2019.

[18] W. Huggins, P. Patil, B. Mitchell, K. B. Whaley, and E. M. Stoudenmire, "Towards quantum machine learning with tensor networks," *Quantum Science and technology*, vol. 4, no. 2, p. 024001, 2019.

[19] M. Cerezo, A. Sone, T. Volkoff, L. Cincio, and P. J. Coles, "Cost function dependent barren plateaus in shallow parametrized quantum circuits," *Nature communications*, vol. 12, no. 1, pp. 1–12, 2021.

[20] H. Wang, Y. Ding, J. Gu, Y. Lin, D. Z. Pan, F. T. Chong, and S. Han, "QuantumNAS: Noise-adaptive search for robust quantum circuits," *arXiv preprint arXiv:2107.10845*, 2021.

[21] R. B. Gómez, C. O'Meara, G. Cortiana, C. B. Mendl, and J. Bernabé-Moreno, "Towards autoqml: A cloud-based automated circuit architecture search framework," *arXiv preprint arXiv:2202.08024*, 2022.

[22] V. Havlíček, A. D. Córcoles, K. Temme, A. W. Harrow, A. Kandala, J. M. Chow, and J. M. Gambetta, "Supervised learning with quantum-enhanced feature spaces," *Nature*, vol. 567, no. 7747, pp. 209–212, 2019.

[23] M. Schuld, A. Bocharov, K. M. Svore, and N. Wiebe, "Circuit-centric quantum classifiers," *Physical Review A*, vol. 101, no. 3, p. 032308, 2020.

[24] E. Farhi and H. Neven, "Classification with quantum neural networks on near term processors," *arXiv preprint arXiv:1802.06002*, 2018.

[25] V. Bergholm, J. Izaac, M. Schuld, C. Gogolin, M. S. Alam, S. Ahmed, J. M. Arrazola, C. Blank, A. Delgado, S. Jahangiri *et al.*, "Pennylane: Automatic differentiation of hybrid quantum-classical computations," *arXiv preprint arXiv:1811.04968*, 2018.

[26] T. Matsumine, T. Koike-Akino, and Y. Wang, "Channel decoding with quantum approximate optimization algorithm," in *2019 IEEE International Symposium on Information Theory (ISIT)*. IEEE, 2019, pp. 2574–2578.

[27] T. Koike-Akino, T. Matsumine, Y. Wang, D. S. Millar, K. Kojima, and K. Parsons, "Variational quantum demodulation for coherent optical multi-dimensional QAM," in *2020 Optical Fiber Communications Conference and Exhibition (OFC)*. OSA, 2020, pp. 1–3.

[28] T. Koike-Akino, P. Wang, and Y. Wang, "Quantum transfer learning for Wi-Fi sensing," *arXiv preprint arXiv:2205.08590*, 2022.

[29] B. Liu, T. Koike-Akino, Y. Wang, and K. Parsons, "Learning to learn quantum turbo detection," *arXiv preprint arXiv:2205.08611*, 2022.

[30] T. Koike-Akino, P. Wang, and Y. Wang, "AutoQML: Automated quantum machine learning for Wi-Fi integrated sensing and communications," *arXiv preprint arXiv:2205.09115*, 2022.

[31] B. Liu, T. Koike-Akino, Y. Wang, and K. Parsons, "Variational quantum compressed sensing for joint user and channel state acquisition in grant-free device access systems," *arXiv preprint arXiv:2205.08603*, 2022.

[32] F. Arute, K. Arya, R. Babbush, D. Bacon, J. C. Bardin, R. Barends, R. Biswas, S. Boixo, F. G. Brandao, D. A. Buell *et al.*, "Quantum supremacy using a programmable superconducting processor," *Nature*, vol. 574, no. 7779, pp. 505–510, 2019.

[33] H.-S. Zhong, H. Wang, Y.-H. Deng, M.-C. Chen, L.-C. Peng, Y.-H. Luo, J. Qin, D. Wu, X. Ding, Y. Hu *et al.*, "Quantum computational advantage using photons," *Science*, vol. 370, no. 6523, pp. 1460–1463, 2020.

[34] E. Farhi, J. Goldstone, and S. Gutmann, "A quantum approximate optimization algorithm," *arXiv preprint arXiv:1411.4028*, 2014.

[35] E. Farhi and A. W. Harrow, "Quantum supremacy through the quantum approximate optimization algorithm," *arXiv preprint arXiv:1602.07674*, 2016.

[36] E. Anschuetz, J. Olson, A. Aspuru-Guzik, and Y. Cao, "Variational quantum factoring," in *International Workshop on Quantum Technology and Optimization Problems*. Springer, 2019, pp. 74–85.

[37] A. Kandala, A. Mezzacapo, K. Temme, M. Takita, M. Brink, J. M. Chow, and J. M. Gambetta, "Hardware-efficient variational quantum eigensolver for small molecules and quantum magnets," *Nature*, vol. 549, no. 7671, pp. 242–246, 2017.

[38] E. R. Miranda, "On interfacing the brain with quantum computers: An approach to listen to the logic of the mind," *arXiv preprint arXiv:2101.03887*, 2020.

[39] M. Swan, "BCI quantum computing IPLD for brain," *ResearchGate preprint:342184271*, Jun. 2020.

[40] V. Gandhi, G. Prasad, D. Coyle, L. Behera, and T. M. McGinnity, "Evaluating quantum neural network filtered motor imagery brain-computer interface using multiple classification techniques," *Neurocomputing*, vol. 170, pp. 161–167, 2015.

[41] W. Hao-Han, J. Fu-Jiang, L. Lian-You, and W. Liang, "A stochastic filtering algorithm using Schrödinger equation," *Acta Automatica Sinica*, vol. 40, no. 10, pp. 2370–2376, 2014.

[42] L. Behera and I. Kar, "Quantum stochastic filtering," in *2005 IEEE International Conference on Systems, Man and Cybernetics*, vol. 3. IEEE, 2005, pp. 2161–2167.

[43] V. Gandhi, G. Prasad, D. Coyle, L. Behera, and T. M. McGinnity, "EEG-based mobile robot control through an adaptive brain–robot interface," *IEEE Transactions on Systems, Man, and Cybernetics: Systems*, vol. 44, no. 9, pp. 1278–1285, 2014.

[44] R. A. Ramadan and A. V. Vasilakos, "Brain computer interface: control signals review," *Neurocomputing*, vol. 223, pp. 26–44, 2017.

[45] A. Pérez-Salinas, A. Cervera-Lierta, E. Gil-Fuster, and J. I. Latorre, "Data re-uploading for a universal quantum classifier," *Quantum*, vol. 4, p. 226, 2020.

[46] M. Schuld, V. Bergholm, C. Gogolin, J. Izaac, and N. Killoran, "Evaluating analytic gradients on quantum hardware," *Physical Review A*, vol. 99, no. 3, p. 032331, 2019.

[47] J. R. McClean, S. Boixo, V. N. Smelyanskiy, R. Babbush, and H. Neven, "Barren plateaus in quantum neural network training landscapes," *Nature communications*, vol. 9, no. 1, pp. 1–6, 2018.

[48] J. Birjandtalab, D. Cogan, M. B. Pouyan, and M. Nourani, "A non-EEG biosignals dataset for assessment and visualization of neurological status," in *2016 IEEE International Workshop on Signal Processing Systems (SiPS)*. IEEE, 2016, pp. 110–114.

[49] U. Orhan, K. E. Hild, D. Erdoğmuş, B. Roark, B. Oken, and M. Fried-Oken, "RSVP keyboard: An EEG based typing interface," in *2012 IEEE International Conference on Acoustics, Speech and Signal Processing (ICASSP)*. IEEE, 2012, pp. 645–648.

[50] A. L. Goldberger, L. A. Amaral, L. Glass, J. M. Hausdorff, P. C. Ivanov, R. G. Mark, J. E. Mietus, G. B. Moody, C.-K. Peng, and H. E. Stanley, "Physiobank, physiotoolkit, and physionet: components of a new research resource for complex physiologic signals," *circulation*, vol. 101, no. 23, pp. e215–e220, 2000.

[51] P. Margaux, M. Emmanuel, D. Sébastien, B. Olivier, and M. Jérémie, "Objective and subjective evaluation of online error correction during P300-based spelling," *Advances in Human-Computer Interaction*, vol. 2012, 2012.

[52] K. J. Miller, D. Hermes, N. Witthoft, R. P. Rao, and J. G. Ojemann, "The physiology of perception in human temporal lobe is specialized for contextual novelty," *Journal of neurophysiology*, vol. 114, no. 1, pp. 256–263, 2015.

[53] K. J. Miller, G. Schalk, D. Hermes, J. G. Ojemann, and R. P. Rao, "Spontaneous decoding of the timing and content of human object perception from cortical surface recordings reveals complementary information in the event-related potential and broadband spectral change," *PLoS computational biology*, vol. 12, no. 1, 2016.

[54] S. Y. Günay, M. Yarossi, D. H. Brooks, E. Tunik, and D. Erdoğmuş, "Transfer learning using low-dimensional subspaces for EMG-based classification of hand posture," in *2019 9th International IEEE/EMBS Conference on Neural Engineering (NER)*. IEEE, 2019, pp. 1097–1100.

[55] K. J. Miller, D. Hermes, F. Pestilli, G. S. Wig, and J. G. Ojemann, "Face percept formation in human ventral temporal cortex," *Journal of neurophysiology*, vol. 118, no. 5, pp. 2614–2627, 2017.